DOI: 10.1002/chem.200600060

A DNA-Binding Copper(I) Metallosupramolecular Cylinder that Acts as an Artificial Nuclease

Laura J. Childs,[b] Jaroslav Malina,[b] Britt Elin Rolfsnes,[d] Mirela Pascu,[a, b] Maria J. Prieto,[c] Mark J. Broome,[b] P. Mark Rodger,[b] Einar Sletten,[d] Virtudes Moreno,*[c] Alison Rodger,*[b] and Michael J. Hannon*[a, b]

Abstract: The DNA binding of a dicationic pyridylimine-based dicopper(I) metallosupramolecular cylinder is reported together with its ability to act as an artificial nuclease. The cylinder binds strongly to DNA; more strongly than the spherical dication $[Ru(phen)_3]^{2+}$ (phen = 1,10-phenanthroline), but more weakly than the corresponding tetracationic cylinders. DNA coiling effects are not observed with this dication, in contrast to the situation with the previously reported tetracationic cylinder involving a similar ligand. Linear dichroism (LD) data suggests that the dicopper cylinder binds in a different orientation from that of the tetracationic iron cylinder. Furthermore, the dicopper cylinder shows DNA-cleavage activity in the presence of peroxide. Of particular note is that the cylinder displays a marked and unusual ability to cleave both DNA strands at the same site, probably reflecting its dinuclear nature and possibly its mode of binding to the DNA.

Keywords: artificial nucleases · bioinorganic chemistry · copper · DNA cleavage · supramolecular chemistry

Introduction

The genetic "code" of most living organisms is contained in their DNA. In mammalian cells, approximately 3 cm of DNA carries the information needed to assemble and sustain the entire organism.[1] Processing of the genetic information (transcription or replication) requires sequence-specific recognition. This is achieved by proteins, most frequently through major-groove binding interactions, as the size and shape of the major groove of B-DNA varies more with base sequence. In addition, this groove contains more hydrogen-bond donor and acceptor sites whose spatial dispositions are sequence dependent. For example, zinc-finger subunits are found in many DNA-binding proteins and contain a zinc ion that holds together a cylindrical loop of amino acids that recognises the DNA major groove.[1,2] Other helical DNA-recognition motifs employed by proteins include α-helices, and such protein recognition of DNA usually occurs through noncovalent interactions. Traditional *synthetic* DNA-recognition agents are generally much smaller than those of proteins and, as a consequence, frequently act through either intercalation or minor-groove binding.[3,4] Synthetic agents that target the DNA major groove by binding through noncovalent interactions have the potential to be powerful agents for sequence-specific DNA recognition. We recently reported the noncovalent DNA binding of syn-

[a] M. Pascu, Prof. M. J. Hannon
School of Chemistry, University of Birmingham
Edgbaston, Birmingham B15 2TT (UK)
Fax: (+44) 121-414-7871
E-mail: m.j.hannon@bham.ac.uk

[b] Dr. L. J. Childs, Dr. J. Malina, M. Pascu, M. J. Broome, Prof. P. M. Rodger, Prof. A. Rodger, Prof. M. J. Hannon
Department of Chemistry, University of Warwick
Coventry, CV4 7AL (UK)
Fax: (+44) 2476-524-112
E-mail: a.rodger@warwick.ac.uk

[c] Dr. M. J. Prieto, Prof. V. Moreno
Departament de Química Inorgànica
Diagonal 647, 08028-Barcelona (Spain)
Fax: (+34) 93-490-7725
E-mail: virtudes.moreno@qi.ub.es

[d] B. E. Rolfsnes, Prof. E. Sletten
Department of Chemistry, University of Bergen
Allgt. 41, 5007 Bergen (Norway)

Supporting information for this article is available on the WWW under http://www.chemeurj.org/ or from the author: Deconvolution of the film LD spectrum to assign Cu-helicate transition polarisations; calculation of the orientation of Cu-helicate on the DNA; DNA-cleavage activity of the cylinders with pBR322 plasmid DNA and hydrogen peroxide; DNA-cleavage activity of the cylinders with ct-DNA and hydrogen peroxide; possible major-groove and minor-groove binding orientations consistent with a 70° binding angle; NMR and ESI-MS data for the copper(I) cylinder.

thetic tetracationic metallosupramolecular cylinders that are similar in size and shape to protein DNA-recognition units.[5] These cylinders target the DNA major groove, spanning five or more base pairs, and induce dramatic intramolecular DNA coiling, which is unprecedented for synthetic agents and, in part, reminiscent of DNA coiling induced by histones in the cell nucleus.

DNA recognition by metal complexes is an area of intense investigation, driven primarily by the GG recognition, believed to be the key to the clinical activity of the metallodrugs cisplatin, carboplatin and oxaliplatin, which are among the most effective clinical anticancer agents.[6] This recognition takes place by the formation of platinum–nitrogen bonds.[7] However, metal complexes are also particularly suited for *noncovalent* approaches[7] and molecular designs, due to 1) the wide range of geometries and structures that metal units can support, 2) the ease of molecular assembly that coordination chemistry can afford, 3) the enhanced polarisation on coordination of hydrogen-bond acceptor and donor residues and, perhaps most importantly, 4) the cationic charge that the metallocentres impart to the reagents, which affords a substantial energetic contribution to the noncovalent binding to anionic DNA.

Examples of metal complexes that exhibit noncovalent interactions[3,8–12] with DNA include the octahedral ruthenium(II) complex $[Ru(phen)_3]^{2+}$ (phen = 1,10-phenanthroline) (although the precise binding modes of the Δ and Λ enantiomers of this compound seem complex)[9] and functionalised analogues that can act as metallointercalators, such as $[Ru(phen)_2(dppz)]^{2+}$ (dppz = dipyridophenazine). Barton has shown that the dppz ligand intercalates between base pairs of the DNA while the two phen ligands reside in a DNA groove,[10] and has recently applied related molecules to detect base-pair mismatches.[12] Nordén et al. reported bisintercalation for the complex $[Ru_2\{\mu\text{-}C4(cpdppz)_2\}(phen)_4]^{4+}$ (cpdppz = cyclopentadipyridophenazine). They suggest that the dppz groups of the molecule intercalate from either the major or minor groove with the bridging chain lying in the opposite groove.[11]

In previous studies[5] we used *tetracationic* cylinders[13] assembled by using metal dications. These cylinders are metallosupramolecular triple helicates,[14] in which three ligand strands are wrapped around two iron(II) centres. The molecular design is based on pyridylimine ligands and the cylinders can be assembled in one-pot reactions from commercial aldehydes, amines and metal salts. This allows the design to be varied systematically.[13,15,16] The various monometal complexes mentioned above are smaller than the dinuclear cylinders that we have developed and afford smaller molecular surfaces that span only two to three DNA base pairs. Moreover, none exhibit the dramatic intramolecular DNA coiling observed with the cylinder. Herein, we now describe the DNA binding of a dinuclear double-helical metallosupramolecular cylinder[16] assembled by copper(I) centres. We were intrigued to explore the effects of using copper(I) cylinders for two reasons. Firstly, the copper(I) cylinders would have a low charge, which might allow us to probe the effect of charge on strength of binding and extent of DNA coiling. Secondly, copper complexes of diimine ligands, such as phenanthroline, are known to exhibit oxidative DNA-cleavage activity that is thought to proceed by means of Fenton-generated hydroxyl-radical or copper-bound oxidants, such as $[CuO]^{+}$ or $[Cu(OH)]^{2+}$[17,18] (and there has been some recent interest[19] in polynuclear analogues). This opens up the exciting possibility that copper(I) cylinders might act as artificial nucleases.

There has been a single report of DNA binding of copper(I) supramolecular double-helicates based on an oligobipyridine unit.[20] Binding to DNA was confirmed, although the precise binding mode was not unambiguously established. The dicationic copper(I) cylinders described herein bind strongly to DNA and do indeed cleave DNA in the presence of an oxidising agent. In contrast to mononuclear copper-containing artificial nucleases, such as the elegant Clip-Phen agents of Meunier,[18] which usually cleave a single DNA strand, these new copper(I) cylinders show a tendency to cleave both DNA strands at the same site.[21]

Results and Discussion

Our previous studies focused on the DNA binding of tetracationic cylinders with a triple-helical architecture formed by three ligand strands (structure **L**) wrapped around two metal dications.[5,13] Reaction of this ligand **L** with mono-

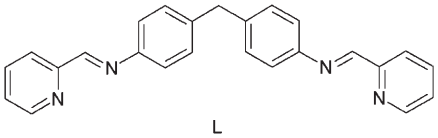

L

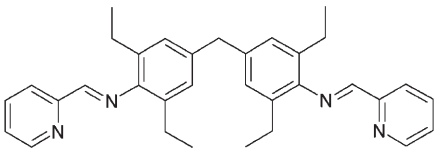

$\mathbf{L^a}$

cations, such as copper(I), leads to dinuclear double-stranded complexes with 2:2 stoichiometry $[M_2\mathbf{L}_2]^{2+}$.[15,16] However, in solution, these complexes are an equilibrium mixture of two dimeric isomers: a helicate (*rac*-isomer) and a metallocyclophane (*meso*-isomer) (Figure 1). To obtain exclusively the helical isomer, we introduced ethyl groups onto the spacer to give ligand $\mathbf{L^a}$.[16]

Addition of ethyl groups to the central spacer destabilises the cyclophane configuration so that only $[M_2(\mathbf{L^a})_2]^{2+}$ helicate species are present in solution. This is evident from the ^{1}H NMR spectrum that reveals a single solution species at

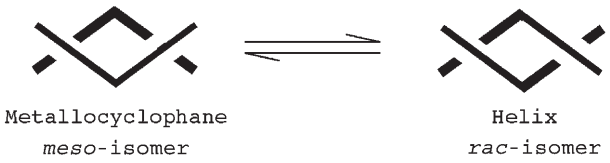

Figure 1. Representation of metallocyclophane (box) and helicate conformations.

room temperature and low temperature, and the central CH_2 resonance that being a singlet confirms the helical conformation (the cyclophane conformation gives rise to two doublets). Electrospray ionisation mass spectrometry (ESI-MS) confirms the dinuclear stoichiometry. The PF_6 salt has been crystallographically characterised and further confirms the double-helicate structure. This double-helical $[Cu_2(\mathbf{L}^a)_2]^{2+}$ cation represents a dicationic cylinder. Before detailing the DNA-binding studies it is pertinent to compare this copper cylinder with the previously studied iron(II), nickel(II) and cobalt(II) triple-stranded cylinders that bind in the major groove and induce the dramatic coiling (Figure 2).[5] These three triple-stranded cylinders are essentially isostructural and distances quoted are for the iron(II) cylinder only. The new copper(I) cylinder and the previously reported iron cylinder are of very similar length. Lengths along the cylinder axis between the extreme carbon atoms or the extreme hydrogen atoms[22] are: for copper 16.6 and 18.5 Å, respectively, and for iron 17.3 and 19.3 Å, respectively. Thus, the copper cylinder is very slightly shorter (~5%). The two cylinders are also similar in radius: for copper, radius-to-carbon is 4.5 Å and radius-to-hydrogen is 5.5 Å, and for iron, radius-to-carbon is 4.3 Å and radius-to-hydrogen is 5.3 Å. Thus, the copper cylinder is slightly wider (~4%). When viewed down the metal–metal axis (Figure 2b) the copper cylinder is more square. Thus, the copper cylinder has very similar dimensions to the iron(II) cylinder, but is slightly different in shape.

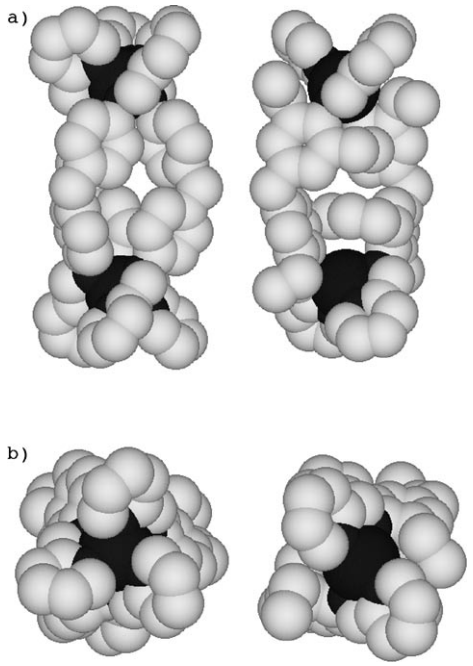

Figure 2. Space-filling side views (a) and end views (b) of the iron(II) cylinder[13] $[Fe_2(\mathbf{L})_3]^{4+}$ (left) and the copper(I) cylinder $[Cu_2(\mathbf{L}^a)_2]^{2+}$ (right); hydrogen atoms are omitted for clarity.

Absorption and circular dichroism spectroscopy: Circular dichroism (CD) was used as an initial screen to confirm the DNA binding of the copper cylinder. The CD and absorption spectra of calf-thymus DNA (ct-DNA) and $[Cu_2(\mathbf{L}^a)_2]^{2+}$ alone and together in solution in different mixing ratios were recorded. The UV-visible absorption spectrum of $[Cu_2(\mathbf{L}^a)_2]^{2+}$ is shown in Figure 3 and reveals absorption bands with maxima at 320 and 480 nm; DNA has no absorbance above 300 nm. All of the spectra of the DNA/$[Cu_2(\mathbf{L}^a)_2]^{2+}$ solutions show cylinder absorption bands consistent with the increasing concentration of the cylinder, however, evidence of light scattering at higher cylinder loadings suggests some degree of DNA condensation or aggregation.

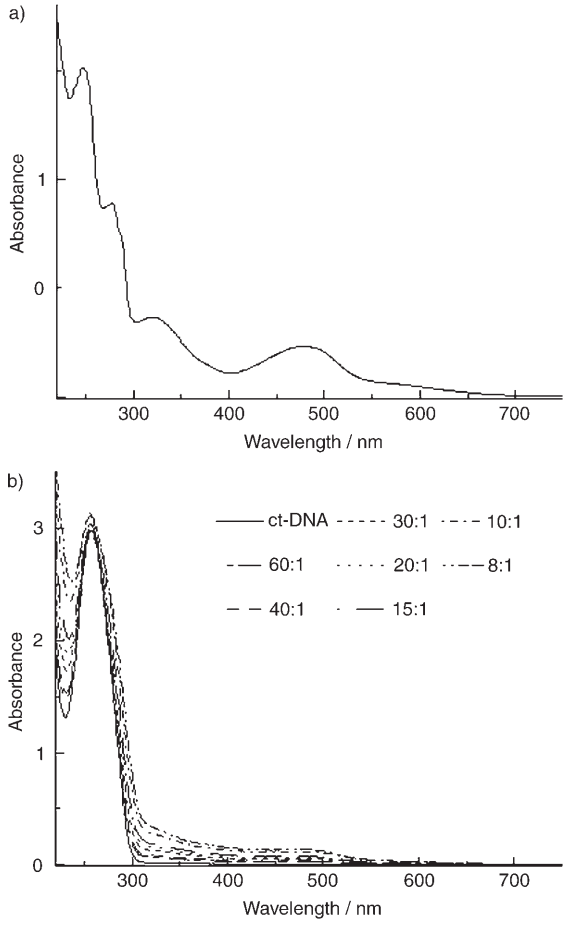

Figure 3. a) Absorption spectrum of 25 μM $[Cu_2(\mathbf{L}^a)_2]^{2+}$ in water. b) Absorption spectra of ct-DNA (500 μM DNA, 10 mM Na cacodylate, 20 mM NaCl) in the presence of $[Cu_2(\mathbf{L}^a)_2]^{2+}$. Mixing ratios ([DNA base]: $[Cu_2(\mathbf{L}^a)_2]^{2+}$]) are indicated. Pathlength = 1 cm.

As expected, $[Cu_2(\mathbf{L}^a)_2]^{2+}$ has no intrinsic CD signal because this compound exists as a racemic mixture of *P* and *M* helices. Therefore, any CD signal above 300 nm corresponding to cylinder absorbances that appears upon the addition of $[Cu_2(\mathbf{L}^a)_2]^{2+}$ to DNA indicates interaction of the metal complex with the chiral DNA, as illustrated in Figure 4. The

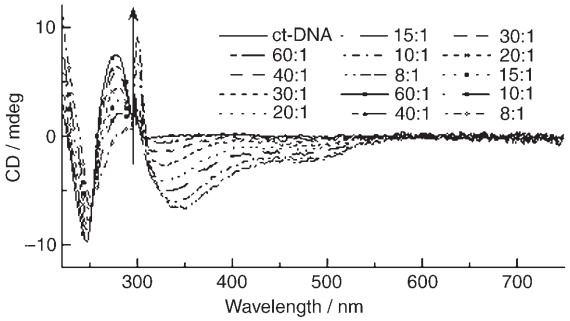

Figure 4. CD spectra of ct-DNA (500 μM DNA, 10 mM Na cacodylate, 20 mM NaCl) in the presence of $[Cu_2(\mathbf{L}^a)_2]^{2+}$ in a 2-mm pathlength (295–220 nm) and in a 1-cm pathlength (750–295 nm). Mixing ratios ([DNA base]:$[Cu_2(\mathbf{L}^a)_2]^{2+}$]) are indicated.

weak, long-wavelength absorbance above 550 nm seen in the absorbance spectrum (Figure 3) is not apparent in the CD spectra. The induced CD (ICD) of the cylinder is negative from long wavelength to 305 nm, then shows a small positive signal from 295–305 nm, is negative from 252–295 nm and positive below this wavelength. The ICD in the DNA region could be due either to the presence of a competing ICD signal (from the cylinder) at the same wavelength, or to a ligand-induced DNA ICD, or to small structural changes in the DNA as a result of the helicate binding. Plots of ICD signal versus concentration of cylinder at 477, 345 and 270 nm (data not shown) all show smooth increases in signal, except for the last two data points in the DNA region, which is where there is evidence in all the spectra of DNA aggregation.

Flow linear dichroism: Linear dichroism (LD) is the difference between the absorption of linearly polarised light that is parallel to a chosen plane and that of linearly polarised light that is perpendicular to the chosen plane and can be used to probe the orientation of molecules. Long molecules, such as DNA (minimum length of ~250 base pairs), can be oriented in a flow Couette cell by viscous drag.[23] The linearly polarised light is incident radial to the flow cell and perpendicular to the flow direction. Small unbound molecules are not orientated in the experiment and show no signal. Similarly, molecules bound randomly to the DNA show no signal. However, molecules bound in a specific orientation with respect to the DNA will give a signal.

A flow LD titration series was carried out while keeping the DNA concentration constant at 500 μM (Figure 5). A negative signal was observed from 220–300 nm for the ct-DNA. This is characteristic of ct-DNA and is due to the base pairs lying approximately perpendicular to the DNA axis.[24] In the absence of DNA, the cylinder shows no signal,

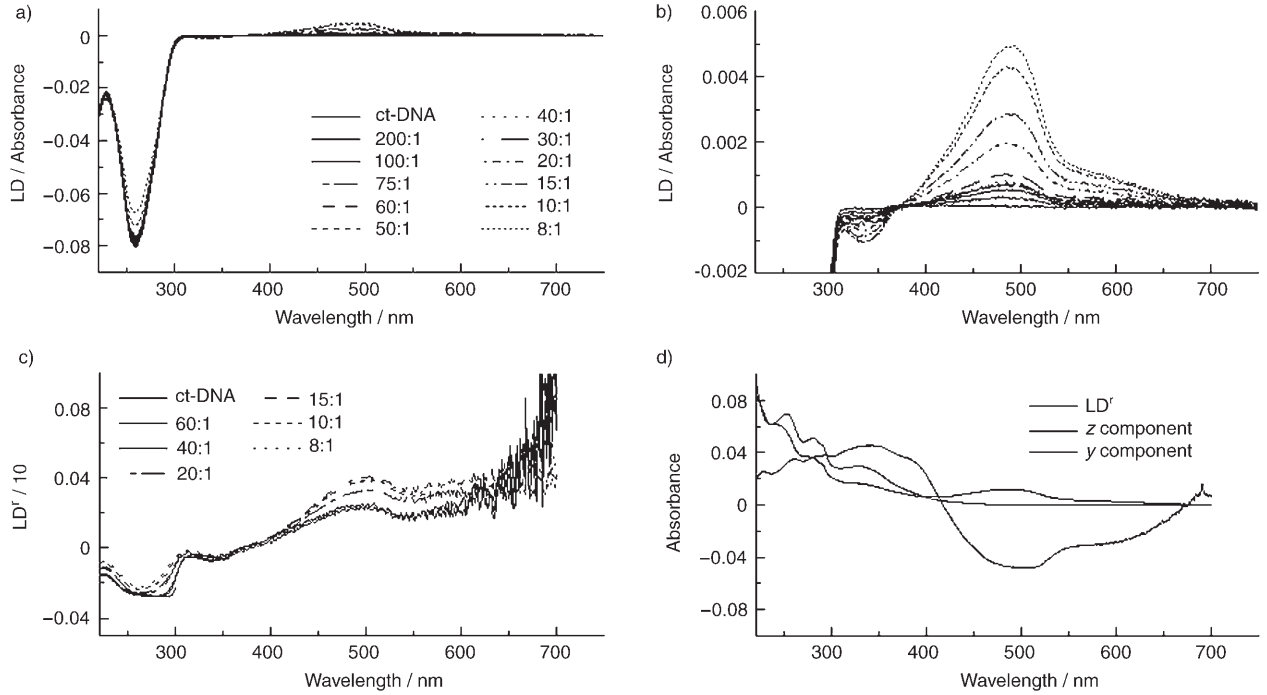

Figure 5. LD spectra of free ct-DNA (500 μM; 10 mM Na cacodylate, 20 mM NaCl) and in the presence of $[Cu_2(\mathbf{L}^a)_2]^{2+}$. Mixing ratios ([DNA base]: $[Cu_2(\mathbf{L}^a)_2]^{2+}$]) are indicated. a) Full scale, b) expanded scale. c) Reduced LD spectra (LD/Absorbance). Beyond 600 nm the absorbance tends to zero and LD^r becomes unreliable. d) Film LD^r spectrum of $[Cu_2(\mathbf{L}^a)_2]^{2+}$ together with those of the *z* (orientation direction, long axis of cylinder) and *y* (perpendicular to *z*, i.e., in the *x*/*y* plane) component spectra.

being too small to be oriented by this flow method. A positive LD signal is observed from 400–700 nm (Figure 5b) upon the addition of $[Cu_2(\mathbf{L}^a)_2]^{2+}$ to the DNA solution and a smaller negative signal is apparent for the in-ligand band at ~340 nm. The presence of these signals confirm that the cylinder is binding to the DNA in a specific orientation(s). As more $[Cu_2(\mathbf{L}^a)_2]^{2+}$ is added, the metal-to-ligand charge-transfer (MLCT) band increases, indicating that more helicate is binding to DNA upon each addition, in accord with the CD data. In contrast to the effect previously observed with the iron helicate, the copper cylinder has little bending effect on the DNA (little or no loss in the DNA signal at ~260 nm confirms DNA still orientated) until a ratio of ~10:1, at which scattering becomes significant in the absorbance and CD spectra (see above). We conclude, therefore, that the copper cylinder does not coil the DNA. The positive LD of the long-wavelength MLCT transition of the cylinder indicates that its transition moments are more parallel than perpendicular to the average DNA axis. By way of contrast, the in-ligand band at ~337 nm is negative and so polarised further from the DNA axis.

Because the DNA is not coiled by the copper cylinder, we can use the DNA LD to determine the orientation of the DNA and, hence, estimate the orientations of the cylinder transition moments on the DNA. The reduced LD (LD^r) is defined in Equation (1) in which α is the angle between the DNA helix axis and the transition moment polarisation and S is the orientation parameter.

$$LD^r = LD/Absorbance = 3S/2(3\cos^2\alpha - 1) \quad (1)$$

The value of α is approximately 86° for the DNA bases,[24] thus, $S \sim 0.18$ in this experiment. To analyse the LD data further, we need to understand something about the spectroscopy of $[Cu_2(\mathbf{L}^a)_2]^{2+}$ itself. To study this, the copper cylinder was immobilised in a polyvinylalcohol (PVA) film that was then stretched. Under such conditions the long axis of the cylinder is preferentially aligned along the stretch direction, allowing component spectra to be determined from the LD data (Figure 5d). The method of deconvolution to component spectra is outlined in the Supporting Information. The long-wavelength MLCT band is almost completely polarised perpendicular to the helicate's long axis. This transition is polarised approximately along the line joining the Cu to the centre of the chelate. By contrast, the in-ligand region of ~340 nm is dominated by transitions moving along the ligands, which couple to give predominantly a transition polarised from the Cu to a point between the ligands. By taking the LD^r values from Figure 5c at the low ligand loading (no scattering; little contribution at 260 nm from cylinder spectroscopy), it follows that the long axis of the copper helicate lies at approximately 70° to the axis of the DNA helix (see Supporting Information for the calculation).

Fluorescence competition-binding assays: Both iron(II) and copper(I) cylinders bind strongly to cellulose,[25] which makes membrane dialysis unsuitable for the determination of binding constants. Therefore, to estimate the strength of binding, an ethidium bromide (EB) competition assay was carried out. This method monitors the displacement of EB from DNA by following the decrease in its fluorescence intensity as it is displaced from DNA into an aqueous environment. The concentrations of DNA and EB were kept constant throughout the experiment at a DNA:EB ratio of 4:5, and $[Cu_2(\mathbf{L}^a)_2]^{2+}$ was added sequentially. The cylinder displaces EB and the EB fluorescence is quenched. At a DNA base:cylinder ratio of about 15:1, the shape of the curve changes, presumably indicating the aggregation of the DNA. This occurs at a lower cylinder loading than in the CCD and LD experiments, because of the bound cationic EB. Thus, the copper cylinder does not completely displace the EB, in contrast to the situation with the iron cylinder. The data in Figure 6 allow us to conclude that the copper cylinder binds more strongly to DNA than does EB or $[Ru(phen)_3]^{2+}$ and less strongly than the iron cylinder. This confirms that (as would be expected) electrostatic charge is an important factor in determining the strength of binding to the anionic DNA (the tetracations bind much more strongly than the dication). Nevertheless, the shape is also a significant factor, with the cylindrical dication exhibiting a higher binding constant than the spherical $[Ru(phen)_3]^{2+}$, despite the fact that the latter will have a higher charge density. Thus, the shape (and the fit on the DNA) of the supramolecular cylinder is indeed important.

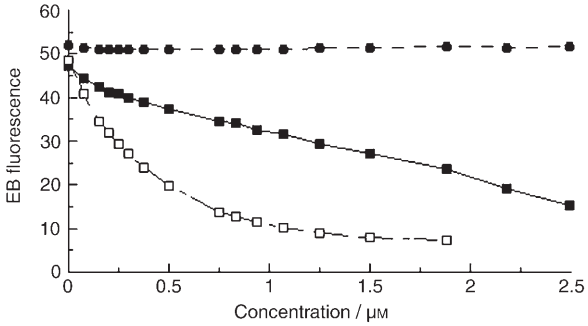

Figure 6. Fluorescence at 593 nm versus concentration of $[Cu_2(\mathbf{L}^a)_2]^{2+}$ (■), $[Fe_2(\mathbf{L})_3]$ (□) and $[Ru(phen)_3]^{2+}$ (●) in the presence of ct-DNA and EB (12 μM DNA, 15 μM EB, 10 mM Na cacodylate, 20 mM NaCl).

NMR studies: NMR titration experiments were performed to try to study the interaction between the copper(I) cylinder and a decamer $d(TATGGCCATA)_2$. Initial experiments involved the decamer (0.35 mM) dissolved in water with 10% of D_2O, 50 mM phosphate buffer and 40 mM NaCl. However, it became clear rapidly that the copper(I) cylinder was not stable in phosphate buffer (thus, phosphate buffer is not used in any of the other experiments described herein). To try to circumvent this problem, a second titration experiment was performed in which the decamer was dissolved in water with 10% D_2O and 30 mM NaCl at pH 5.95, at duplex concentration 0.4 mM. A 36 mM solution of the cylinder in 100% $[D_6]$DMSO was added to achieve a cylinder:duplex

ratio of 1:1. Although the cylinder was stable under these conditions, the addition led simply to precipitation of a red-brown solid that did not redissolve in water or aqueous methanol with ultrasound or heating. It seems likely that the cylinder precipitates the DNA at the concentrations required for NMR studies, which is consistent with the results at high loading ratios in the more-dilute CD, LD and UV-visible studies.

Artificial nuclease activity: To assess DNA-cleavage activity the interaction of the cylinder with pUC19 plasmid DNA was studied. Gel electrophoresis (1% agarose gel) was used to visualise the effects (Figure 7). Incubation was for one

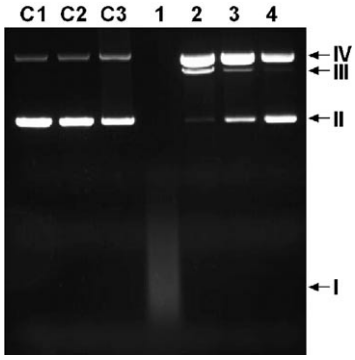

Figure 7. Gel electrophoresis of plasmid pUC19 after being incubated with $[Cu_2(\mathbf{L}^a)_2]^{2+}$ and hydrogenperoxide (HP). Lane C1, nonmodified plasmid; lane C2, plasmid with HP (hydrogen peroxide); lane C3, plasmid with $[Cu_2(\mathbf{L}^a)_2]^{2+}$ at 10:1 (base:cylinder) ratio; lanes 1—4, plasmid with HP and modified with $[Cu_2(\mathbf{L}^a)_2]^{2+}$ at different mixing ratios of 10:1, 20:1, 40:1 and 100:1, respectively. Band I, short fragments of DNA; band II, supercoiled plasmid; band III, linearised plasmid; band IV, relaxed plasmid. [HP] = 6.6 mM; [DNA] = 250 μM.

hour at 37 °C. The plasmid (lane C1) contains predominantly supercoiled DNA (band II) with small amounts of relaxed DNA (band IV). Addition of the cylinder to this plasmid DNA resulted in very little change in the gel chromatogram (lane C3). Similarly, addition of peroxide to the DNA caused no change (lane C2). However, addition of both cylinder and peroxide (lane 4) led to a reduction in supercoiled DNA (band II) and a corresponding increase in relaxed DNA (band IV). Relaxation of the supercoiling requires nicking of a single strand and, thus, implies that cylinder-induced DNA-strand scission occurs under these conditions. Increasing the concentration of cylinder (lanes 2, 3) leads to a further increase in relaxed DNA and a decrease in supercoiled DNA. Intriguingly, a band (band III) corresponding to linearised DNA (arising from cleavage of both strands at the same site) is apparent even in lane 4, well before the supercoiled DNA has disappeared. This is unusual (normally supercoiled DNA almost disappears before the formation of linear DNA) and could be explained as follows: 1) the complex has more than one reactive centre and cuts both DNA strands simultaneously; or 2) after the first cut, the complex stays bound and cuts the second strand; or 3) the binding of the copper cylinder is cooperative, leading to double-strand breaks. Although it is hard to be definitive, it seems that the ratios of the double-strand and single-strand breaks are independent of concentration, suggesting that the third proposal is unlikely. The first explanation is an attractive one, given the two-fold symmetry of the copper cylinder and the approximate two-fold symmetry of the DNA helix.

If the concentration of the cylinder is further increased (Figure 7, lane 1) the DNA is cleaved into short fragments (band I) that have high mobility within the gel. Control samples (free ligand with and without peroxide; and simple copper(II) chloride and hexafluorophosphate salts with and without peroxide) confirm that the complex is essential for cleavage. Very similar results were obtained with pBR322 plasmid (see Supporting Information).

A similar gel electrophoresis experiment with ct-DNA (a linear, polymeric DNA, as used in the spectroscopic experiments) confirmed that the effect is not merely restricted to circular DNAs. After addition of cylinder and peroxide to the ct-DNA, the bands corresponding to long DNA (closer to the loading well) disappeared, and only fast-running, short DNA fragments were observed (see Supporting Information).

Further confirmation of the DNA cleavage comes from linear dichroism experiments. As described, addition of the cylinder to ct-DNA has no effect on the DNA LD. Solutions incubated over periods of a few hours show no loss in DNA LD signal. However, if peroxide is added to the cylinder-DNA solution there is a fairly rapid loss of the DNA LD signal, consistent with cleavage of the ct-DNA into small fragments that can no longer be oriented in the flow cell. Peroxide alone has no effect on the ct-DNA LD signal.

Visual conformation of the DNA-cleavage activity comes from molecular-level images of the pBR322 plasmid DNA and copper(I) cylinder, obtained by using tapping-mode atomic force microscopy (AFM) (Figure 8). Plasmid samples incubated for one hour with cylinder alone show no evidence of strand scission (Figure 8a, b), whereas the sample incubated with 6 μM copper(I) cylinder and hydrogen peroxide shows clear evidence of DNA-strand scission to give linear fragments (Figure 8c). This effect is even more dramatic upon addition of a higher concentration of copper(I) cylinder (20 μM) to the DNA (Figure 8d). In this case, we observe just short pieces of DNA as a result of the cleavage activity. Extended incubation times led to small fragments even at lower cylinder concentration.

Conclusion

The results obtained with this dicationic copper(I) cylinder cast further light on the role of charge in the binding and coiling of DNA by tetracationic cylinders.

Charge is important in binding (as expected), and tetracationic cylinders bind more strongly than this dicationic cylinder. Indeed, electrostatic forces will be important in designing noncovalent DNA-recognition agents that bind

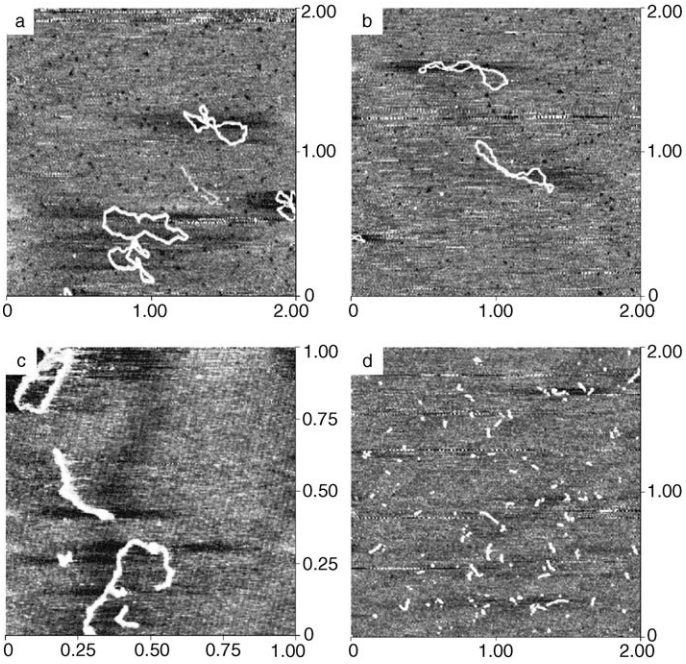

Figure 8. pBR322 DNA with (a) 6 μM copper(I) cylinder, (b) 20 μM copper(I) cylinder, (c) 6 μM copper(I) cylinder with H_2O_2 and (d) 20 μM copper(I) cylinder with H_2O_2. All samples were incubated for 1 hr at 20°C. The dimensions are in μm.

strongly to DNA. However, the molecular shape is also important, with the cylindrical dication exhibiting stronger binding than spherical $[Ru(phen)_3]^{2+}$, despite a lower charge density. This validates our original hypothesis[5] that benefits could be accrued by scaling up from small molecules to designing supramolecular arrays with size and shape similar to nature's own DNA-recognition motifs. The results also imply that charge may be important in the DNA bending and coiling observed with the tetracationic iron(II) cylinder. Our dicationic copper(I) cylinder does not cause such coiling. Charge has been proposed as an important factor in DNA-bending processes[26] and indeed is believed to play a role in DNA coiling about histones. The copper cylinder induces DNA aggregation (leading to precipitation) at mixing ratios much lower than those for the tetracationic cylinders, despite its lower binding constant, and this may be related to the lack of observed intramolecular DNA coiling (in the intramolecular coils the cylinders are wrapped up by the DNA, so they cannot bridge between and aggregate DNA molecules).

The copper cylinder binds to DNA without disturbing its B-DNA configuration. Based on the size of the cylinder and the pitch of the DNA, a cylinder lying perfectly along the major groove would make an angle between its long axis and the axis of the DNA helix of around 60°. The observed average binding angle (~70°) of this copper(I) cylinder would, therefore, be consistent with binding in the major groove or with a minor-groove binding mode (which, due to the cylinder size, might involve lying outside the minor groove, perhaps with partial insertion of the cylinder into the groove). Support for this comes from a preliminary molecular-dynamics simulation[27] of poly-d(AT)$_2$ focused on configurations in which the cylinder made angles of 70° (±5°) with the DNA axis. This revealed several binding modes in which the cylinder sat nicely in the major groove, together with one configuration outside the minor groove. These potential binding modes are visualised in images provided in the Supporting Information, although these are not intended to imply definitive binding modes.

Interestingly, this copper cylinder exhibits DNA-cleavage activity in the presence of peroxide. The cylinder exhibits an unusual tendency to perform a double-strand cleavage at the same site, possibly reflecting its dinuclear nature. The cleavage ability extends the potential applications of these metallosupramolecular cylinders, opening up the possibility of using copper-based cylinders as artificial nucleases. Studies are currently underway to impart sequence selectivity to the cylinder systems for this purpose.

Experimental Section

Materials: Ultrapure water (18.2 MΩ) was used in all experiments. The ct-DNA (highly polymerised) was purchased from Sigma-Aldrich and was dissolved in water without any further purification. Stock solutions of ct-DNA were kept frozen until the day of use. DNA solutions were prepared as required from the frozen samples by diluting to the desired concentration of polynucleotide with a buffer of 10 mM cacodylate (prepared from sodium cacodylate adjusted to pH 6.8 with hydrochloric acid) and 20 mM NaCl. The DNA concentrations were determined spectroscopically by using the known molar-extinction coefficient of $\varepsilon_{258} = 6600\ mol^{-1}\,dm^3\,cm^{-1}$ per DNA base.[28] Commercially available tris-acetate-EDTA (TAE, from Fisher) working buffer was used for gel electrophoresis of pUC19 plasmid DNA (New England Biolabs). The gel loading buffer was prepared by dissolving 0.25% (w/v) of xylene cyanole, 0.25% (w/v) of bromophenol blue and 30% (w/v) of glycerol in water.

Preparation of ligand L^a: This was prepared by mixing two equivalents of pyridine-2-carboxyaldehyde and one equivalent of 4,4′-methylene-bis(2,6-diethylaniline) in methanol as previously reported.[16] Preparation of the chloride salt of the copper(I) complex was analogous to that of the corresponding PF_6 salt, which has been characterised crystallographically:[16] $[Cu_2(\mathbf{L}^a)_2][Cl]_2$ was prepared by mixing ligand **L^a** and copper(I) chloride in a 1:1 ratio in methanol. The dark-red solution was heated under reflux overnight and then cooled to RT. The solvent was removed by rotary evaporation and the red solid was dried over P_2O_5. ^{1}H NMR (MeOH, 298 K): $\delta = 8.79$ (s, 1H; H_i), 8.62 (d, $J = 4.5$ Hz, 1H; H_6), 8.28, (t, $J = 7.3$ Hz, 1H; $H_{4/5}$), 8.14 (d, $J = 7.5$ Hz, 1H; H_3), 7.87 (br dd, $J = 7.0$, 5.3 Hz, 1H; $H_{4/5}$), 7.07 (br s, 1H; H_{Ph}), 6.57 (br s, 1H; H_{Ph}), 3.87 (s, 1H; central CH_2), 2.73 (br m, 1H; CH_2), 2.64 (br m, 1H; CH_2), 2.21 (br m, 1H; CH_2), 2.04 (br m, 1H; CH_2), 1.04 (br s, 3H; CH_3), 0.56 ppm (br s, 3H; CH_3); UV/Vis (H_2O): λ_{max} (ε) = 258 (6600), 478 (9450), 321 (14800), 278 nm (36800 $mol^{-1}\,dm^3\,cm^{-1}$); ESI-MS (MeOH): m/z: 552 $[Cu_2(\mathbf{L}^a)_2]^{2+}$.

Circular dichroism: Spectra were collected in cuvettes of pathlength 2 mm and 1 cm by using a Jasco J-715 spectropolarimeter. Spectroscopic titrations were performed from which CD and UV/Vis absorption spectra were recorded. Titrations were carried out at constant concentrations of DNA (500 μM), NaCl (20 mM) and sodium cacodylate buffer (10 mM). The ratio of DNA:metal complex was decreased during the titration series by incrementing the concentration of metal complex in the cuvette from 0–62.5 μM. Two stock solutions were prepared. The first was of metal complex in water (500 μM) and the second solution contained DNA (1000 μM), NaCl (40 mM) and sodium cacodylate buffer (20 mM). After the addition of x cm^3 of the metal-complex solution to the cuvette, an equivalent volume of the second DNA stock solution was added. This

meant that the concentrations of DNA, NaCl and sodium cacodylate buffer in the cuvette remained unaltered.[29]

Linear dichroism: Flow LD spectra were collected by using a flow Couette cell in a Jasco J-715 spectropolarimeter adapted for LD measurements. Long molecules, such as DNA (minimum length of ~250 base pairs), can be orientated in a flow Couette cell. The flow cell consists of a fixed outer cylinder and a rotating solid quartz inner cylinder, separated by a gap of 0.5 mm, giving a total pathlength of 1 mm.[23,29]

Stretch film is used to orient small molecules and involves dissolving the molecule of interest in a polymer solution, such as polyvinylalcohol (PVA). A 10% (w/v) low-molecular-weight PVA solution in water (4.8 cm^3) was prepared and heated to near boiling to ensure that all the PVA had dissolved. The solution was cooled and a saturated aqueous solution of metal complex (0.2 cm^3) added. The viscous solution was then cast onto a glass plate and left to dry in a ventilated, dust-free environment. A blank film was also prepared by adding water (0.2 cm^3) instead of metal complex to the PVA solution. When dry, both films were carefully peeled from the glass plate by using a scalpel and were then placed in a mechanical stretcher. Under gentle heating the films were stretched by a factor of two. The UV/Vis and LD spectra of both films were recorded and the spectra of the blank film was subtracted from that of the metal-complex film. It was then possible to calculate component spectra (see Supporting Information).

Fluorescence competition assay: An ethidium bromide (EB) competition-binding assay was carried out according to a modified literature method[30] by using a Perkin–Elmer LS-50B spectrofluorimeter.

Gel electrophoresis: All electrophoresis experiments were carried out by using a Pharmacia GNA-100 submarine unit. Gel trays of 110×100 mm were used, with an 11-toothed comb to produce the sample wells. A Pharmacia Electrophoresis Power Supply, ECPS-3000, was used as a constant voltage supply set to 70 V and 65 mA. The volume of agarose solution to be used was calculated so as to produce a gel with a depth of 4 mm. TAE working buffer was used for the gel electrophoresis. Gels were stained with ethidium bromide visualised under a UV lamp and were photographed by using a UVP white/UV transilluminator. The samples were prepared by mixing the metal complex with DNA in different ratios, keeping the DNA concentration constant at 2.5×10^{-4} M. For the DNA cleavage studies, all samples were incubated for 1 hr at 37°C in 1 mM sodium cacodylate and 20 mM NaCl prior to analysis by gel electrophoresis.

Atomic force microscopy:[31] AFM images of pBR322 plasmid DNA were collected by using two different concentrations of copper(I) cylinder (6 and 20 μM). DNA–metal-complex adducts were prepared as follows: pBR322 DNA was incubated in an appropriate volume with the required metal complex in 2-[4-(2-hydroxyethyl)-1-piperazinyl]ethanesulfonic acid (HEPES) buffer (HEPES 4 mM pH 7.4, KCl 5 mM, $MgCl_2$ 2 mM). All solutions were prepared with water (18.2 MΩ) that had been filtered through 0.2 nm FP030/3 filters (Schleider and Schuell, Germany) and centrifuged at 4000 g several times to avoid salt deposits and to provide a clear background upon imaging. The samples were left to equilibrate at 37°C for 30 min in the dark. Samples were prepared for AFM by placing a drop (6 μL) of DNA–metal-complex adduct solution onto mica (Ashville–Schoonmaker Mica, Newport News, VA). After adsorption for 5 min at RT, the samples were rinsed for 10 s in a jet of deionised water (18 MΩ cm^{-1} Milli-Q water) directed from a squeeze bottle onto the surface. The samples were blow-dried with compressed argon over silica gel and then imaged by using a Nanoscope III Multimode AFM (Digital Instrumentals, Santa Barbara, CA) operating in tapping mode in air at a scan rate of 1–3 Hz. The AFM probes were 125 μm long monocrystalline silicon cantilevers with integrated conical-shaped Si tips.

Acknowledgements

We thank the Leverhulme Trust (Grant F/125/BC) and the EU (MARCY RTN HPRN-CT-2002-00175; Marie Curie fellowship HPMF-CT-2002-01856) for support. This work was conducted within the framework of COST D20 (metal complexes in anticancer and antiviral therapy), working group D2O/0010/02 (noncovalent DNA recognition), which supported an exchange of researchers (B.E.R.). We thank the EPSRC National Mass Spectrometry Service Centre, Swansea, for recording electrospray mass spectra. M.J.H. is the Royal Society of Chemistry Sir Edward Frankland Fellow 2004–2005.

[1] J. M. Berg, J. L. Tymoczko, L. Stryer, *Biochemistry*, Freeman, New York, **2002**; S. Neidle, *Nucleic Acid Structure and Function*, Oxford University Press, Oxford, **2002**.

[2] C. Brandon, J. Tooze, *Introduction to Protein Structure*, Garland, New York, **1998**.

[3] P. B. Glover, P. R. Ashton, L. J. Childs, A. Rodger, M. Kercher, R. M. Williams, L. De Cola, Z. Pikramenou, *J. Am. Chem. Soc.* **2003**, *125*, 9918–9919; corrigendum: P. K. L. Fu, P. M. Bradley, C. Turro, *Inorg. Chem.* **2003**, *42*, 878–884; corrigendum: *Inorg. Chem.* **2004**, *43*, 2220; C. L. Kielkopf, K. E. Erkkila, B. P. Hudson, J. K. Barton, D. C. Rees, *Nat. Struct. Biol.* **2000**, *7*, 117–121; I. Greguric, J. R. Aldrich-Wright, J. G. Grant Collins, *J. Am. Chem. Soc.* **1997**, *119*, 3621–3622; J. L. Kisko, J. K. Barton, *Inorg. Chem.* **2000**, *39*, 4942–4949; G. Bobba, J. C. Frias, D. Parker, *Chem. Commun.* **2002**, *8*, 890–891; G. Colmenarejo, A. Holmen, B. Nordén, *J. Phys. Chem. B* **1997**, *101*, 5196–5204.

[4] C. Melander, D. M. Herman, P. B. Dervan, *Chem. Eur. J.* **2000**, *6*, 4487–4497; P. B. Dervan, *Bioorg. Med. Chem.* **2001**, *9*, 2215.

[5] M. J. Hannon, V. Moreno, M. J. Prieto, E. Molderheim, E. Sletten, I. Meistermann, C. J. Isaac, K. J. Sanders, A. Rodger, *Angew. Chem.* **2001**, *113*, 903–908; *Angew. Chem. Int. Ed.* **2001**, *40*, 880–884; I. Meistermann, V. Moreno, M. J. Prieto, E. Molderheim, E. Sletten, S. Khalid, P. M. Rodger, J. Peberdy, C. J. Isaac, A. Rodger, M. J. Hannon, *Proc. Natl. Acad. Sci. USA* **2002**, *99*, 5069–5074; E. Molderheim, M. J. Hannon, I. Meistermann, A. Rodger, E. Sletten, *J. Biol. Inorg. Chem.* **2002**, *7*, 770–780; M. J. Hannon, A. Rodger, *Pharmaceutical Visions*, **2002**, *Autumn Issue*, 14–16; A. Oleski, A. G. Blanco, R. Boer, I. Usón, J. Aymami, A. Rodger, M. J. Hannon, Miquel Coll, *Angew. Chem.* **2006**, *118*, 1249–1253; *Angew. Chem. Int. Ed.* **2006**, *45*, 1227–1231.

[6] B. Lippert, *Cisplatin, Chemistry and Biochemistry of A Leading Anticancer Drug*, Wiley-VCH, Weinheim, **1999**; J. Reedijk, *Chem. Commun.* **1996**, 801–806; Z. J. Guo, P. J. Sadler, *Adv. Inorg. Chem.* **2000**, *49*, 183–306; J. D. Roberts, J. Peroutka, N. Farrell, *J. Inorg. Biochem.* **1999**, *77*, 51–57; S, J. Lippard, J. M. Berg, *Principles of Bioinorganic Chemistry*, University Science Books, Mill Valley, CA, **1994**.

[7] Cisplatin binds to the DNA bases through coordination bonds (not covalent bonds), yet the binding is in some ways analogous to that of DNA alkylating agents, such as nitrogen mustards, with which they are classified clinically. With the term "noncovalent" binding by metal complexes used herein we are formally referring to noncovalent binding that does not involve direct coordination of the metal centre to atoms on the DNA molecule.

[8] K. K. Patel, E. A. Plummer, M. Darwish, A. Rodger, M. J. Hannon, *J. Inorg. Biochem.* **2002**, *91*, 220–229; J. Aldrich-Wright, C. Brodie, E. C. Glazer, N. W. Luedtke, L. Elson-Schwab, Y. Tor, *Chem. Commun.* **2004**, 1018–1019; S. E. Wellman, D. B. Sittman, J. B. Chaires, *Biochemistry* **1994**, *33*, 384–388.

[9] C. V. Kumar, J. K. Barton, N. J. Turro, *J. Am. Chem. Soc.* **1985**, *107*, 5518–5523; C. Hiort, B. Nordén, A. Rodger, *J. Am. Chem. Soc.* **1990**, *112*, 1971–1982; M. Eriksson, M. Leijon, C. Hiort, B. Nordén, A. Graslund, *J. Am. Chem. Soc.* **1992**, *114*, 4933–4934.

[10] K. E. Erkkila, D. T. Odom, J. K. Barton, *Chem. Rev.* **1999**, *99*, 2777–2795.

[11] B. Önfelt, P. Lincoln, B. Nordén, *J. Am. Chem. Soc.* **2001**, *123*, 3630–3637.

[12] U. Schatzschneider, J. K. Barton, *J. Am. Chem. Soc.* **2004**, *126*, 8630–8631; E. Ruba, J. R. Hart, J. K. Barton, *Inorg. Chem.* **2004**, *43*, 4570–4578.

[13] M. J. Hannon, C. L. Painting, A. Jackson, J. Hamblin, W. Errington, *Chem. Commun.* **1997**, 1807–1808.
[14] J.-M. Lehn, *Supramolecular Chemistry: Concepts and Perspectives*, VCH, Weinheim, **1995**; C. Piguet, G. Bernardinelli, G. Hopfgartner, *Chem. Rev.* **1997**, *97*, 2005–2062; M. Albrecht, *Chem. Rev.* **2001**, *101*, 3457–3497; M. J. Hannon, L. J. Childs, *Supramol. Chem.* **2004**, *16*, 7–22.
[15] M. J. Hannon, C. L. Painting, N. W. Alcock, *Chem. Commun.* **1999**, 2023–2024; L. J. Childs, N. W. Alcock, M. J. Hannon, *Angew. Chem.* **2001**, *113*, 1113–1115; *Angew. Chem. Int. Ed.* **2001**, *40*, 1079–1080; L. J. Childs, N. W. Alcock, M. J. Hannon, *Angew. Chem.* **2002**, *114*, 4418–4421; *Angew. Chem. Int. Ed.* **2002**, *41*, 4244–4247.
[16] L. J. Childs, M. Pascu, A. J. Clarke, N. W. Alcock, M. J. Hannon, *Chem. Eur. J.* **2004**, *10*, 4291–4300.
[17] D. S. Sigman, T. W. Bruice, A. Mazumder, C. L. Sutton, *Acc. Chem. Res.* **1993**, *26*, 98–104.
[18] a) M. Pitie, B. Donnadieu, B. Meunier, *Inorg. Chem.* **1998**, *37*, 3486–3489; b) M. Pitie, C. Boldron, H. Gornitzka, C. Hemmert, B. Donnadieu, B. Meunier, *Eur. J. Inorg. Chem.* **2003**, 528–540.
[19] S. T. Frey, H. H. J. Sun, N. N. Murthy, K. D. Karlin, *Inorg. Chim. Acta* **1996**, *242*, 329–338; K. J. Humphreys, K. D. Karlin, S. E. Rokita, *J. Am. Chem. Soc.* **2002**, *124*, 6009–6019; K. J. Humphreys, K. D. Karlin, S. E. Rokita, *J. Am. Chem. Soc.*, **2002**, *124*, 8055–8066; C. Tu, Y. Shao, N. Gan, D. Xu, Z. J. Guo, *Inorg. Chem.* **2004**, *43*, 4761–4766.
[20] B. Schoentjes, J.-M. Lehn, *Helv. Chim. Acta* **1995**, *78*, 1–12.
[21] Although mononuclear complexes usually favour single-strand cleavage, double-strand cleavage is sometimes also possible: See, for example, ref. [18b] and P. U. Maheswari, S. Roy, H. den Dulk, S. Barends, G. van Wezel, B. Kozlevcar, P. Gamez, J. Reedijk, *J. Am. Chem. Soc.* **2006**, *128*, 710–711.
[22] Lengths quoted are the distances between the centroids of the three pyridine C5 atoms at each end of the helix or the three pyridine H5 atoms. Radii are taken perpendicular to the helix axis.
[23] A. Rodger, B. Norden, *Circular and Linear Dichroism*, Oxford University Press, Oxford, **1997**.
[24] P.-J. Chou, W. C. Johnson, *J. Am. Chem. Soc.* **1993**, *115*, 1205–1214.
[25] M. J. Hannon, I. Meistermann, C. J. Isaac, C. Blomme, J. Aldrich-Wright, A. Rodger, *Chem. Commun.* **2001**, 1078–1079.
[26] L. J. Maher, III, *Curr. Opinion Chem. Biol.* **1998**, *2*, 688–694; I. Rouzina, A. Bloomfield, *Biophys. J.* **1998**, *84*, 3152–3564.
[27] These initial simulations are used merely to visualise how a 70° binding angle might appear. Detailed molecular-dynamics simulations and their analysis are beyond the scope of this current study, but will be described in a future report. For details of a related molecular-dynamics simulation of the iron(II) cylinder on DNA see S. Khalid, A. Rodger, M. J. Hannon, P. M. Rodger, *Chem. Eur. J.* **2006**, *12*, 3493–3506
[28] R. D. Wells, J. E. Larson, R. C. Grant, B. E. Shortle, C. R. Cantor, *J. Mol. Biol.* **1970**, *54*, 465–497.
[29] A. Rodger, *Methods Enzymol.* **1993**, *226*, 232–258.
[30] A. McCoubrey, H. C. Latham, P. R. Cook, A. Rodger, G. Lowe, *FEBS Lett.* **1996**, *380*, 73–78.
[31] G. B. Onoa, G. Cervantes, V. Moreno, M. J. Prieto, *Nucleic Acids Res.* **1998**, *26*, 1473–1480.

Received: January 16, 2006
Published online: April 27, 2006

